JOURNAL OF BACTERIOLOGY, Aug. 1998, p. 4258–4269 Vol. 180, No. 16
0021-9193/98/$04.00+0

Physiological Control and Regulation of the *Rhodobacter capsulatus cbb* Operons

GEORGE C. PAOLI,† PADUNGSRI VICHIVANIVES, AND F. ROBERT TABITA*

Department of Microbiology and Plant Molecular Biology/Biotechnology Program, The Ohio State University, Columbus, Ohio 43210-1292

Received 8 January 1998/Accepted 3 June 1998

The genes encoding enzymes of the Calvin-Benson-Bassham (CBB) reductive pentose phosphate pathway in *Rhodobacter capsulatus* are organized in at least two operons, each preceded by a separate *cbbR* gene, encoding potential LysR-type transcriptional activators. As a prelude to studies of *cbb* gene regulation in *R. capsulatus*, the nucleotide sequence of a 4,537-bp region, which included $cbbR_{II}$, was determined. This region contained the following open reading frames: a partial *pgm* gene (encoding phosphoglucomutase) and a complete *qor* gene (encoding NADPH:quinone oxidoreductase), followed by $cbbR_{II}$, *cbbF* (encoding fructose 1,6-bisphosphatase), *cbbP* (encoding phosphoribulokinase), and part of *cbbT* (encoding transketolase). Physiological control of the CBB pathway and regulation of the *R. capsulatus cbb* genes were studied by using a combination of mutant strains and promoter fusion constructs. Characterization of mutant strains revealed that either form I or form II ribulose 1,5-bisphosphate carboxylase/oxygenase (RubisCO), encoded by the *cbbLS* and *cbbM* genes, respectively, could support photoheterotrophic and autotrophic growth. A strain with disruptions in both *cbbL* and *cbbM* could not grow autotrophically and grew photoheterotrophically only when dimethyl sulfoxide was added to the culture medium. Disruption of *cbbP* resulted in a strain that did not synthesize form II RubisCO and had a phenotype similar to that observed in the RubisCO-minus strain, suggesting that there is only one *cbbP* gene in *R. capsulatus* and that this gene is cotranscribed with *cbbM*. Analysis of RubisCO activity and synthesis in strains with disruptions in either $cbbR_I$ or $cbbR_{II}$, and β-galactosidase determinations from wild-type and mutant strains containing cbb_{Ip}- and cbb_{IIp}-*lacZ* fusion constructs, indicated that the cbb_I and cbb_{II} operons of *R. capsulatus* are within separate CbbR regulons.

Purple nonsulfur photosynthetic bacteria display exceptional metabolic versatility (20, 31) and assimilate CO_2 via the highly regulated Calvin-Benson-Bassham (CBB) reductive pentose phosphate pathway (12, 17, 48). During photo- and chemoautotrophic growth, CO_2 is the sole source of cellular carbon, and maximal levels of the key CBB pathway enzymes, ribulose 1,5-bisphosphate carboxylase/oxygenase (RubisCO) and phosphoribulokinase (PRK), are observed (48). Photoheterotrophic growth results in much lower yet substantial levels of RubisCO and PRK; however, under these conditions the CBB pathway functions primarily to help maintain the redox balance of the cell by allowing CO_2 to serve as an electron sink. Alternate electron acceptors such as dimethyl sulfoxide (DMSO) can function in place of CO_2 (7, 43, 56).

The organization and regulation of structural genes encoding enzymes of the CBB pathway have been extensively studied in *Rhodobacter sphaeroides*, and there are at least three major operons which comprise the *cbb* regulon of this organism. Two major operons, the cbb_I, or form I, operon and the cbb_{II}, or form II, operon, are comprised of structural genes of the CBB pathway, some of which are duplicated (13–15). The third operon consists of the *cbbXYZ* genes, encoding two proteins of unknown function and phosphoglycolate phosphatase, respectively, and is downstream of the cbb_I operon (18). Transcription of both the cbb_I and cbb_{II} operons is positively regulated by the product of the *cbbR* gene, which is upstream and divergently transcribed from the *R. sphaeroides* cbb_I operon (16). By contrast, the form I RubisCO genes (*cbbLS*) of *R. capsulatus* are not associated with any CBB pathway structural genes (38, 39), and an open reading frame (ORF) with sequence similarity to *cbbQ*, which is also downstream of *cbbLS* of *Pseudomonas hydrogenothermophila* and *Chromatium vinosum* (62), is found downstream of *R. capsulatus cbbLS* (38). The *cbbQ* gene product has no known function in *R. capsulatus* (20a). In addition, there are two *cbbR* genes in *R. capsulatus*; $cbbR_I$ is upstream and divergently transcribed from the *cbbLS* genes (38), while $cbbR_{II}$ is upstream and divergently transcribed from the *cbbFPTGAM* genes (39).

The recent description of variant *cbb* gene organization in *R. capsulatus* and *R. sphaeroides*, particularly the presence of two *cbbR* genes in *R. capsulatus*, suggests potential differences in *cbb* gene regulation. For example, unlike *R. sphaeroides*, *R. capsulatus* does not synthesize form I RubisCO when the organism is grown photoheterotrophically on malate (39, 46). Furthermore, the *R. capsulatus* form I enzyme is immunologically distinct from the form I enzyme of *R. sphaeroides* (15, 39) and appears to have been acquired by horizontal gene transfer (38). Thus, to initiate and provide a framework for *cbb* gene regulation studies in *R. capsulatus*, specific *cbb* gene disruption strains and *cbb* promoter fusions were constructed and characterized.

MATERIALS AND METHODS

Bacterial strains, plasmids, media, and growth conditions. Plasmids and *R. capsulatus* strains used or constructed are listed in Table 1. *Escherichia coli* JM107 (60), JM109 λpir, and S17-1 λpir (40) were grown aerobically on LB medium (2) at 37°C. Aerobic cultures of *R. capsulatus* were grown in PYE medium (57) at 30°C. Photosynthetic cultures were grown in Ormerod's medium (37) supplemented with thiamine (1 μg/ml), nicotinic acid (1 μg/ml), and biotin (0.1 μg/ml). Photo- and chemoautotrophic growth conditions were previously

* Corresponding author. Mailing address: Department of Microbiology and Plant Molecular Biology/Biotechnology Program, The Ohio State University, 484 West 12th Ave., Columbus, OH 43210-1292. Phone: (614) 292-4297. Fax: (614) 292-6337. E-mail: Tabita.1@osu.edu.

† Present address: Air Force Research Laboratory/MLQR, Tyndall Air Force Base, FL 32403-5323.

TABLE 1. Plasmids and bacterial strains used this study

Plasmid or strain	Relevant characteristics; phenotype[a]	Reference
Plasmids		
pK18, pK19	Km^r, pUC derivatives	42
pTZ18R	Ap^r, pUC derivative	33
pUC1318	Ap^r, pUC derivative with modified multiple cloning site	21
pUC1813	Ap^r, pUC derivative with modified multiple cloning site	21
pRL648	Km^r Ap^r, pUC derivative with the Tn*5* Km^r gene cassette	6
pRK415	Tc^r, broad-host-range cloning vector, *lacZ*α	22
pRPS-1	Tc^r, broad-host-range expression vector containing *R. rubrum cbbM* promoter and *cbbR* gene in pRK404	7
pRPSKm	Km^r derivative of pRPS-1	8a
pJP5603	Km^r, mobilizable suicide vector	40
pTC5603	Tc^r derivative of pJP5603	This work
pHP45Ω	Ap^r Sp^r, containing Ω cassette encoding Sp^r	41
pVK101	Tc^r Km^r, broad-host-range vector	23
pUC1318K	Ap^r Km^r, pUC1318 with a 1.5-kb *Hin*dIII-*Sal*I fragment from Tn*5* encoding Km^r	35
pUC1813K	Ap^r Km^r, pUC1813 with a 1.5-kb *Sal*I fragment from pUC1318K encoding the Tn*5* Km^r	This work
pXBA601	Tc^r, broad-host-range *lacZ* translational fusion vector	1
pRCFII	*R. capsulatus* cosmid library clone containing the cbb_{II} genes	39
pK18FIIEH	pK18 containing the *R. capsulatus* $cbbR_{II}$, *cbbF*, *cbbP*, *cbbT*, *cbbG*, and *cbbA* genes on an 8.4-kb *Eco*RI-*Hin*dIII fragment from pRCFII	This work
pRKFIIEH	pRK415 containing the *Eco*RI-*Hin*dIII fragment from pK18FIIEH	This work
pRKFIP	pRK415 with a 9-kb *Pst*I fragment containing the *R. capsulatus* $cbbR_I$, *cbbLS*, and *cbbQ* genes	39
pUC1813::FIB	pUC1813 containing the *R. capsulatus cbbLS* genes on a 4.7-kb *Bam*HI fragment from pRKFIP	This work
pUC1813::FIΩ	pUC1318::FIB Δ *Eco*RI::Sp^r	This work
pJP::FIΩ	pJP5603 containing the *Bam*HI insert of pUC1813::FIΩ	This work
pK18FIIS2-I	pK18 containing the *R. capsulatus cbbM* gene on a 2-kb *Sal*I fragment	39
pUC1318FII	pUC1318 containing the *R. capsulatus cbbM* gene cloned on a 2-kb *Sal*I fragment	This work
pUC1318::FIIKm	pUC1318FII with the Δ *Hin*dIII::Km^r cartridge inserted	This work
pTC::FIIKm	pTC5603 with the *Sal*I fragment of pUC1318::FIIKm	This work
pK18FIIB2.3	pK18 with a 2.3-kb *Bam*HI fragment containing the *R. capsulatus* $cbbR_{II}$, *cbbF*, and *cbbP* genes	39
pK18FIIBSm	pK18 containing part of *R. capsulatus cbbP* on a 543-bp *Bam*HI-*Sma*I fragment	This work
pK18CBBPΩ	pK18FIIBSm with the Sp^r cartridge from pHP45Ω cloned into the *Sal*I site of *cbbP*	This work
pJP::CBBPΩ	pJP5603 containing the *cbbP*::Ω interposon of pK18CBBPΩ cloned as a *Hin*dIII-*Eco*RI fragment	This work
pK18FIIS4.4	pK18 with a 4.4-kb *Sal*I fragment containing the 5′ end of the *R. capsulatus* cbb_{II} cluster	39
pTZ::FII3.7	pTZ18R containing the *R. capsulatus* $cbbR_{II}$ and *cbbF* genes on a 3.7-kb *Sal*I-*Sma*I fragment from pK18FIIEH	This work
pTZ::CbbRKm	pTZ::FII3.7 with a Km^r gene cartridge cloned into the *Bam*HI site of $cbbR_{II}$	This work
pTCTZ::CbbRKm	pTZ::CbbRKm cloned into vector pTC5603 by linearizing with *Xba*I	This work
pJN940A	The *R. sphaeroides* $cbbP_I$ gene cloned as an *Ava*I fragment into pK18	36a
pUC1813::RsP_I	pUC1813 containing the *R. sphaeroides* $cbbP_I$ gene cloned as a 1-kb *Ava*I fragment from plasmid pJN940A	This work
pRPS::RsP_IA	pRPSKm containing the *R. sphaeroides* $cbbP_I$ gene cloned from pUC1813::RsP_I as an *Xba*I fragment	This work
pRPS::RsP_IB	pRsP_IA containing the *Xba*I insert in the opposite orientation	This work
pUC1813S4.4	pUC1813 containing the *R. capsulatus* $cbbR_{II}$, *cbbF*, and *cbbP* genes on a 4.4-kb *Sal*I fragment	This work
pEULA4	4-kb *Eco*RI fragment containing *R. capsulatus cbbL*, $cbbR_I$, *anfA*, and uncharacterized sequence between $cbbR_I$ and *anfA* in pK19	38
pVK::CbbRI	pVK101 containing the the 4-kb *Eco*RI fragment from pEULA4	This work
pVK::CbbRII	4.4-kb *Sal*I fragment containing the *R. capsulatus* $cbbR_{II}$, *cbbF*, and *cbbP* genes cloned into the *Xho*I site of pVK101	This work
pEULA4Ω	pEULA4 with a *Sma*I Sp^r cassette cloned into the unique *Ssp*I site within $cbbR_I$	This work
pJPLA4Ω	pJP5603 containing the $cbbR_I$::Sp^r *Eco*RI fragment from pEULA4Ω	This work
pK18FISN	pK18 containing the 3.2-kb *Sal*I-*Nco*I fragment from pEULA4 such that the *cbbL* start codon is fused to *lacZ*α	This work
pXLB	pXBA601 containing the 3.2-kb *Bam*HI fragment from pK18FISN, cbb_{Ip} fusion to *lacZ*	This work
pXLBP	pXBA601 containing the 367-bp *Pst*I-*Bam*HI fragment from pK18FISN, cbb_{Ip} fusion to *lacZ*	This work
pK18FIISN	pK18 containing the 2.44-kb *Sal*I-*Nco*I fragment from pK18FIIS4.4 such that the *cbbF* start codon is fused to *lacZ*α	This work
pXFB	pXBA601 containing the 722-bp *Bam*HI fragment from pK18FIISN, cbb_{IIp} fusion to *lacZ*	This work
R. capsulatus strains		
SB1003	Rif^r derivative of strain B10; PH^+ PA^+ CA^+	61
SBI$^-$	*cbbL*::Sp^r derivative of SB1003; PH^+ PA^+ CA^+	This work
SBII$^-$	*cbbM*::Km^r derivative of SB1003; PH^+ PA^+ CA^+	This work
SBI-II	*cbbL*::Sp^r, *cbbM*::Km^r derivative of SB1003; PH^- PA^- CA^-	This work
SBP$^-$	*cbbP*::Sp^r derivative of SB1003; PH^- PA^- CA^-	This work
SBRI$^-$	$cbbR_I$::Sp^r derivative of SB1003; PH^+ PA^+ CA^+	This work
SBRII$^-$	$cbbR_{II}$::Km^r derivative of SB1003; PH^+ PA^- CA^-	This work

[a] Ability of strains to grow under various conditions: PH, photoheterotrophically with malate; PA, photoautotrophically; CA, aerobic chemoautotrophically.

described (38, 39). Antibiotic concentrations used for *R. capsulatus* strains were as follows: rifampin, 100 μg/ml; kanamycin, 5 μg/ml; spectinomycin, 10 μg/ml; and tetracycline, 2 μg/ml for plasmid maintenance or 0.1 μg/ml for screening during gene disruption experiments. For *E. coli*, antibiotic concentrations were 30 μg/ml for kanamycin, 50 μg/ml for spectinomycin, 12.5 μg/ml for tetracycline, and 200 μg/ml for trimethoprim. DMSO was used at 30 mM.

DNA manipulations. Routine DNA manipulations, including plasmid preparation, restriction endonuclease digestion, agarose gel electrophoresis, fragment

ligation, and bacterial transformation, were performed by standard methods (2). *R. capsulatus* chromosomal DNA was prepared as previously described (19). For gene disruption experiments, plasmid pJP5603 derivatives were conjugated into *R. capsulatus* SB1003 by using *E. coli* S17-1 λpir (40). For complementation of mutant strains, plasmids were conjugated into *R. capsulatus* by triparental matings on filter pads as previously described (57), using the helper plasmid pRK2013 (10).

Southern blotting and hybridization. Southern transfer experiments were performed by using GeneScreen Plus (NEN, DuPont, Boston, Mass.) or Hybond N+ (Amersham, Arlington Heights, Ill.) membranes. Hybridizations were conducted according to the protocols provided by NEN, DuPont, using formamide under stringent conditions. Probes were labeled with [α-^{32}P]dCTP (NEN, DuPont) by the random prime labeling method (9), using a kit purchased from United States Biochemical Corporation (Cleveland, Ohio).

DNA sequencing and analysis. Nucleotide sequences were determined with an ABI Prism 310 Genetic Analyzer. A thermal cycler and dye terminator cycle sequencing kit were used as described by the manufacturer (Perkin-Elmer, Foster City, Calif.). The M13/pUC forward 23-base primer, M13 reverse (−48) primer, and sequence-specific synthetic primers were used to complete the double-stranded sequence. Sequence analysis was carried out with the University of Wisconsin Genetics Computing Group software, the EGCG extension programs (The Sanger Centre, Hinxton, England), and the MacVector sequence analysis software (International Biotechnology, Inc., New Haven, Conn.).

Preparation of cell extracts and enzyme assays. Culture samples (20 to 30 ml) were taken in late log phase (A_{660} = 0.9 to 1.2) and washed twice in cold buffer (100 mM Tris-HCl, 1 mM EDTA [pH 8.0]) before freezing at −70°C. Thawed pellets were resuspended in 1 ml of TEM buffer (50 mM Tris-HCl, 1 mM EDTA, 5 mM β-mercaptoethanol [pH 7.5]) and disrupted by sonication in an ice bath. Cell debris was removed by centrifugation for 10 min in a microcentrifuge at 4°C.

RubisCO activity was measured as ribulose 1,5-bisphosphate-dependent $^{14}CO_2$ fixation into acid-stable 3-phosphoglycerate (14). PRK was assayed as previously described (47) except that ribulose 5-phosphate was not added directly but generated from ribose 5-phosphate by the addition of 5 U of phosphoriboisomerase (Sigma Chemical, St. Louis, Mo.).

β-Galactosidase was measured by continuous assays in Z buffer (50 mM sodium phosphate [pH 7.0], 10 mM KCl, 1 mM $MgSO_4$, 50 mM β-mercaptoethanol) (36) containing 0.8 mg of *o*-nitrophenol β-D-galactopyranoside (ONPG) per ml. The production of *o*-nitrophenol from ONPG was measured by monitoring the increase in A_{405}. β-Galactosidase activities were calculated by using an extinction coefficient for *o*-nitrophenol of 3.1×10^3 cm^2/mmol (55).

Protein concentrations were determined by a modified Lowry procedure (32) using bovine serum albumin as a standard.

Western immunoblot analysis. Antibodies raised against *R. sphaeroides* form II RubisCO and form I PRK (PRK I) were used to detect *R. capsulatus* form II RubisCO and PRK, respectively. Although *R. capsulatus* form I RubisCO reacts poorly with antibody raised against *R. sphaeroides* form I RubisCO, anti-*Synechococcus* strain PCC 6301 RubisCO antibody cross-reacts well (38, 39) and was used to detect *R. capsulatus* form I RubisCO. Proteins were resolved by sodium dodecyl sulfate polyacrylamide gel electrophoresis (SDS-PAGE) (28). After SDS-PAGE, the proteins were transferred to polyvinylidene difluoride membranes (Immobilon-P; Millipore, Bedford, Mass.), using a Bio-Rad Transblot semidry cell (Bio-Rad, Hercules, Calif.) and established protocols (50). The blots were developed by using the Vistra ECF fluorescent detection system (Amersham Corporation, Buckinghamshire, England) and visualized with a Molecular Dynamics Storm 840 imaging system (Molecular Dynamics, Sunnyvale, Calif.).

Construction of mutant strains. *R. capsulatus* strains with disruptions in *cbbL*, *cbbM*, *cbbP*, *cbbR*$_I$, and *cbbR*$_{II}$ were constructed by mobilizing the appropriate pJP5603 derivative into strain SB1003 from *E. coli* S17-1 λpir. Homologous recombination of the plasmid-borne disrupted gene into the wild-type copy in the chromosome was forced because pJP5603 does not replicate in *R. capsulatus*. Recombinant strains were selected by aerobic growth on PYE plates supplemented with the antibiotic corresponding to the disrupting cassette. Rifampin was used to select against the *E. coli* donor. Resistant clones were screened for sensitivity to the plasmid-encoded antibiotic resistance marker to identify strains that may had undergone a second recombination event. Double recombination was confirmed by Southern blotting and hybridization analysis of chromosomal DNA from the mutant and wild-type strains (data not shown). Specific plasmid and strain constructions are described below.

Strain SBI$^-$ (*cbbL*). A 4.7-kb *Bam*HI fragment, containing the *R. capsulatus cbbLS* genes, was cloned from pRKFIP into pUC1813. The resulting plasmid, pUC1813::FIB, lacked any *Eco*RI sites in the multiple cloning region so that the 639-bp *Eco*RI fragment within *cbbL* could be removed and replaced by the spectinomycin resistance (Sp^r) gene from pHP45Ω. The 6.5-kb *Bam*HI fragment containing the disrupted gene was moved from pUC1813::FIΩ to pJP5603, resulting in plasmid pJP::FIΩ. Plasmid pJP::FIΩ was mobilized into *R. capsulatus* SB1003 from *E. coli* S17-1 λpir. Six of the Sp^r exconjugants screened were sensitive to kanamycin (Km^s). Southern blot analysis of chromosomal DNA prepared from the six Sp^r Km^s isolates revealed that five of them resulted from double recombination. One of these strains was used for subsequent experiments.

Strain SBII$^-$ (*cbbM*). The 2-kb *Sal*I fragment encoding the *R. capsulatus cbbM* gene was cloned from plasmid pK18FIIS2-I into plasmid pUC1318. The resulting construct, pUC1318FII, lacked *Hin*dIII sites within its multiple cloning region. To generate a Km^r cassette with flanking *Hin*dIII sites, a 1.4-kb *Sal*I fragment encoding the Tn*5* Km^r gene was cloned from pUC1318K into plasmid pUC1813, generating pUC1813K. The 650-bp *Hin*dIII fragment within the *cbbM* gene in vector pUC1318FII was removed and replaced by the *Hin*dIII fragment containing the Tn*5* Km^r gene from plasmid pUC1813K. The resulting *cbbM* deletion fragment was cloned as an *Xba*I fragment into plasmid pTC5603, yielding pTC::FIIKm. *E. coli* S17-1 λpir was used to mobilize pTC::FIIKm into *R. capsulatus* SB1003. Three hundred Km^r clones were screened for tetracycline sensitivity (Tc^s). All of the exconjugants were sensitive to 2 μg of tetracyline per ml, but only five clones were sensitive to 0.1 μg/ml. Due to the very low resistance to tetracycline, the 300 clones were examined for loss of pTC5603 by colony hybridization. The five Tc^s clones did not hybridize to the pTC5603 probe, but the 295 Tc^s clones did hybridize to the probe. Three of the five Tc^s clones were screened by Southern blot hybridization analysis of chromosomal DNA and found to be the result of double recombination. One of these recombinants was used for subsequent experiments.

Strain SBI-II (*cbbL cbbM*). To construct a strain lacking genes for both forms of RubisCO, the *cbbM* deletion plasmid pTC::FIIKm was mobilized into *R. capsulatus cbbL* strain SBI$^-$. Two hundred Km^r colonies were screened, and two were Tc^s. Both of these Tc^s clones had lost the pTC5603 vector as determined by colony hybridization using pTC5603 as a probe. Southern blot analysis using *cbbM* and *cbbL* probes revealed that these strains were the result of double recombination, leaving behind a deletion within the chromosomal copy of *cbbM*, with the *cbbL* gene deletion still present.

Strain SBP$^-$ (*cbbP*). A 543-bp *Sma*I-*Bam*HI fragment encoding part of the *R. capsulatus cbbP* gene was cloned from pK18FIIB2.3 into pK18, resulting in plasmid pK18::BSm. The *cbbP* gene was disrupted by cloning the Sp^r gene from pHP45Ω as a *Sal*I fragment into the unique *Xho*I site within the *cbbP* gene fragment in plasmid pK18::BSm, yielding plasmid pK18CBBPΩ. The resulting disrupted gene fragment was cloned as a *Bam*HI-*Sma*I fragment into pJP5603, yielding plasmid pJP::CBBPΩ. *E. coli* S17-1 λpir was used to mobilize plasmid pJP::CBBPΩ into *R. capsulatus* SB1003. Two hundred fifty Sp^r exconjugants were screened, and seven were Km^s. One of these strains was screened by Southern blot hybridization analysis of the chromosomal DNA and found to be the result of a double recombination. This strain, SBP$^-$, was characterized further.

Strain SBRI$^-$ (*cbbR*$_I$). The Sp^r cassette from pHP45Ω was cloned as a *Sma*I fragment into the unique *Ssp*I site within the *cbbR*$_I$ gene in plasmid pEULA4 to yield pEULA4Ω. The *cbbR*$_I$ disruption was cloned from pEULA4Ω into the *Eco*RI site in pJP5603. The resulting plasmid, pJPLA4Ω, was mobilized into *R. capsulatus* SB1003 via *E. coli* S17-1 λpir. Of the 1,500 Sp^r colonies screened, 35 were Km^s. Chromosomal DNA was prepared from eight Km^s clones, and Southern blot and hybridization analysis confirmed that each of the clones was the result of double recombination. One strain, SBRI$^-$, was characterized further.

Strain SBRII$^-$ (*cbbR*$_{II}$). The 3.7-kb *Sal*I-*Sma*I fragment containing the *R. capsulatus cbbR*$_{II}$ and *cbbF* genes was cloned from pK18FIIS4.4 into plasmid pTZ18R, generating pTZ::FII3.7. Removal of the *Sal*I-*Sma*I fragment from the multiple cloning region of pTZ18R during the construction of pTZ::FII3.7 deleted the *Bam*HI site. This allowed disruption of the *cbbR*$_{II}$ gene in pTZ::FII3.7 by insertion of a *Bam*HI fragment containing the Tn*5* Km^r gene from plasmid pRL648 into the unique *Bam*HI site within *cbbR*$_{II}$. The resulting construct, pTZ::CBBRKm, was linearized with *Xba*I and ligated to *Xba*I-digested pTC5603, resulting in plasmid pTZTC::CBBRKm. This plasmid was mobilized into *R. capsulatus* SB1003 from *E. coli* S17-1 λpir. Three hundred Km^r colonies were screened, and 299 were sensitive to Tc. Hybridization of colony blots from the 300 Km^r clones using a probe derived from the Tc^r region of pTC5603 (*Eco*RI to *Pvu*II fragment of pBR322) revealed that only the single Tc^r clone contained the Tc^r gene. Chromosomal DNA was prepared from three of the Tc^s and the Tc^r clone. The Tc^r clone was the result of a single recombination of pTZTC::CBBRKm into the SB1003 chromosome, and each of the three Tc^s clones was the result of double recombination. One of the Km^r Tc^s double-recombinant clones, strain SBRII$^-$, was used in subsequent experiments.

Construction of *cbb* promoter fusions. The translational fusion vector pXBA601 (1) was used for construction of *cbbL* (*cbb*$_{1p}$) and *cbbF* (*cbb*$_{II p}$) promoter fusions to *lacZ*. pXBA601 requires that the fusion end of the promoter fragment be ligated to the unique *Bam*HI site within this vector. For construction of the *cbb*$_{1p}$ fusion, the ends of a 3.2-kb *Sal*I-*Nco*I fragment from pEULA4 were filled with the Klenow fragment of DNA polymerase I. The blunt-ended fragment was cloned into the *Sma*I site of pK18, yielding plasmid pK18FISN. This resulted in an in-frame fusion of the *cbbL* ATG initiation codon that is within the *Nco*I recognition site to *lacZ*. After screening for the proper orientation, the fusion was confirmed by sequencing. A *Pst*I-*Bam*HI fragment and a *Bam*HI fragment were cloned from pK18FISN into pXBA601, resulting in constructs with 367 bp and 3.2 kb upstream of the *cbbL* initiation codon fused to *lacZ*, pXLBP and pXLB, respectively. Inserts were detected by colony blot hybridization, and the orientation of the insert in pXLB was determined by restriction enzyme digestion. The *cbb*$_{II p}$ fusion was constructed by first filling the ends of the 2.44 kb *Sal*I-*Nco*I fragment from plasmid pKFIIS4.4 with the Klenow fragment of DNA polymerase I and ligating it to *Sma*I-cut pK18, yielding pK18FIISN. After screening for the orientation of the insert, the fusion was confirmed by nucleotide

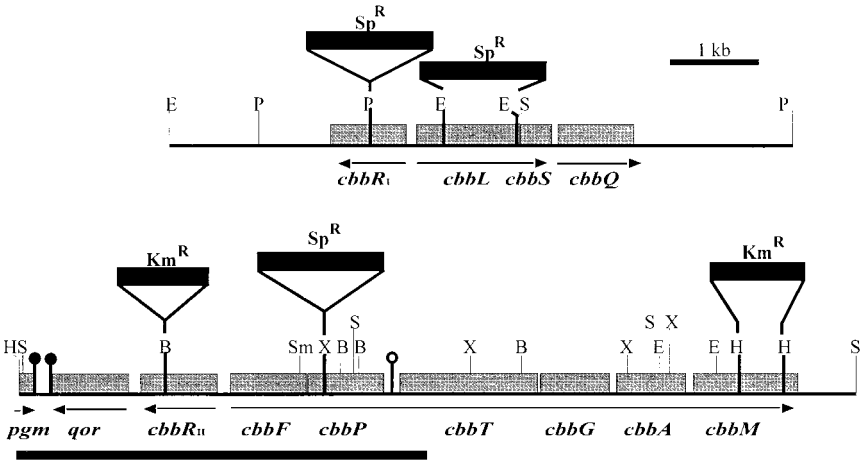

FIG. 1. Map of *R. capsulatus cbb* genes. Arrows indicate direction and size of potential transcripts. The sites of gene disruptions in the mutant strains are indicated. The dark bar denotes the region that was sequenced for this study. ●, potential transcriptional terminator hairpin structure; ♀, hairpin preceded by an RNase E recognition sequence. Gene designations are as follows: *cbbR*, LysR-type transcriptional regulator; *cbbL*, form I RubisCO large subunit; *cbbS*, form I RubisCO small subunit; *cbbQ*, gene of unknown function; *pgm*, phosphoglucomutase; *qor*, NAD(P)H quinone oxidoreductase; *cbbF*, fructose 1,6-sedoheptulose 1,7-bisphosphatase; *cbbP*, phosphoribulokinase; *cbbT*, transketolase; *cbbG*, glyceraldehyde 3-phosphate dehydrogenase; *cbbA*, fructose 1,6-bisphosphate aldolase; *cbbM*, form II RubisCO. Restriction sites: B, *Bam*HI, E, *Eco*RI, H, *Hin*dIII; S, *Sal*I; Sm, *Sma*I, X, *Xho*I.

sequencing. This resulted in an in-frame *lacZ* fusion to the *cbbF* ATG initiation codon that is within the *Nco*I recognition site. A 722-bp *Bam*HI fragment was subcloned from pK18FIISN into pXBA601. The presence of an insert was determined by colony blot hybridization, and the orientation of the insert was determined by nucleotide sequencing. The resulting construct, pXFB, contained 722 bp upstream of *cbbF* fused to *lacZ* at the *cbbF* start codon.

Nucleotide sequence accession number. The nucleotide sequences reported in this paper have been submitted to the GenBank database under accession no. U87282.

RESULTS

Nucleotide sequence analysis and amino acid sequence comparisons. The DNA upstream of the presumptive *R. capsulatus* cbb_{II} operon contains at least two regions of interest with respect to *cbb* gene regulation: the $cbbR_{II}$ gene, encoding a putative *cbb* transcriptional activator, and the $cbbR_{II}$-*cbbF* intergenic region, containing the presumptive cbb_{II} operon promoter. As a prelude to further studies of *R. capsulatus cbb* gene regulation, the nucleotide sequence of a 4,537-bp region, from the *Sal*I site 1.4 kb downstream of $cbbR_{II}$ to the 5′ end of $cbbT_{II}$, was determined (Fig. 1). In addition to $cbbR_{II}$, *cbbF*, *cbbP*, and part of the *cbbT* gene known to be present in this region (39), database searches revealed one full-length ORF and one partial ORF downstream of $cbbR_{II}$. One end of the sequenced region contained a partial ORF (Fig. 1) encoding 83 amino acids that were 56.6% identical (74.7% similar) to the C-terminal portion of *Agrobacterium tumefaciens* phosphoglucomutase and 49.4% identical (69.9% similar) to the human PGM *1+ isoform of phosphoglucomutase (Fig. 2A). A phosphoglucomutase gene had not been previously identified in nonsulfur purple photosynthetic bacteria. An ORF encoding a 322-amino-acid gene product was directly downstream from $cbbR_{II}$ (Fig. 1). The deduced amino acid sequence of this ORF showed 47.7 and 43.3% identity to the NAD(P)H quinone oxidoreductase (QOR) from *Pseudomonas aeruginosa* and *E. coli*, respectively. QOR from *E. coli* has been crystallized (49), and every residue known to be involved in substrate binding or catalysis is conserved in the *R. capsulatus* enzyme (Fig. 2B). The AXXGXXG sequence (Fig. 2B) is an unusual nucleotide binding fingerprint motif found only among the QORs (49).

The CbbR proteins comprise a family of LysR-type transcriptional activators that are involved in the regulation of *cbb* genes, from which they are usually divergently transcribed (17). The *R. capsulatus* $cbbR_{II}$ gene is immediately upstream and divergently transcribed from *cbbF* (Fig. 1). A second *cbbR* gene, $cbbR_{I}$, was found upstream and divergently transcribed from the *R. capsulatus cbbLS* genes (38). Amino acid sequence comparisons and phylogenetic analyses of the *R. capsulatus* CbbR proteins with other CbbRs, presented elsewhere (38), showed that *R. capsulatus* CbbR II is most homologous to *R. sphaeroides* CbbR (55.2% identity) and less homologous to the *R. capsulatus* CbbR I (42.5% identity).

The *R. capsulatus cbbF* gene product is most similar to the fructose 1,6-bisphosphatases (FBPases) from *R. sphaeroides*, showing 84.0% identity with *R. sphaeroides* FBPase II and 66.8% identity to *R. sphaeroides* FBPase I (Fig. 2C). It has been suggested, by analogy to the *R. sphaeroides* cbb_{II} operon, that the *R. capsulatus cbbF* promoter may control the entire *cbbFP TGAM* (cbb_{II}) gene cluster (39). In this respect, it is interesting that three potential CbbR binding sites (17) are present upstream of *cbbF* (sequence not shown).

The *R. capsulatus cbbP* gene, encoding a putative PRK, was immediately downstream of *cbbF* (Fig. 1). A potential ribosome binding site was 8 nucleotides upstream of the *cbbP* start codon and within the $cbbF_{II}$ coding region; thus, *cbbF* and *cbbP* may be translationally coupled and are almost certainly cotranscribed. This arrangement is similar to that of *R. sphaeroides* $cbbF_{I}$-$cbbP_{I}$ (14) and $cbbF_{II}$-$cbbP_{II}$ (13). The predicted molecular weight, 33,244, is very similar to the subunit molecular weight determined for purified *R. capsulatus* PRK (47). *R. capsulatus* PRK is highly similar to *R. sphaeroides* PRK I (86.2% identity) and PRK II (87.0% identity) (Fig. 2D). The domains involved in ATP (24, 25) and pyridine nucleotide (3, 13) binding are indicated in Fig. 2D. Residues implicated by site-directed mutagenesis of the *R. sphaeroides* PRK I in sugar phosphate binding (44) and catalysis (3) are also noted.

The 46 N-terminal amino acids of the *cbbT* gene are encoded by 138 nucleotides at the 3′ end of the sequenced region (Fig. 1). Over this portion of the protein, the *R. capsulatus cbbT* gene product is more similar to *R. sphaeroides* CbbT (91.3% identity) than to *R. capsulatus* TktA (69.6% identical), a second transketolase found in *R. capsulatus* (4) (Fig. 2E).

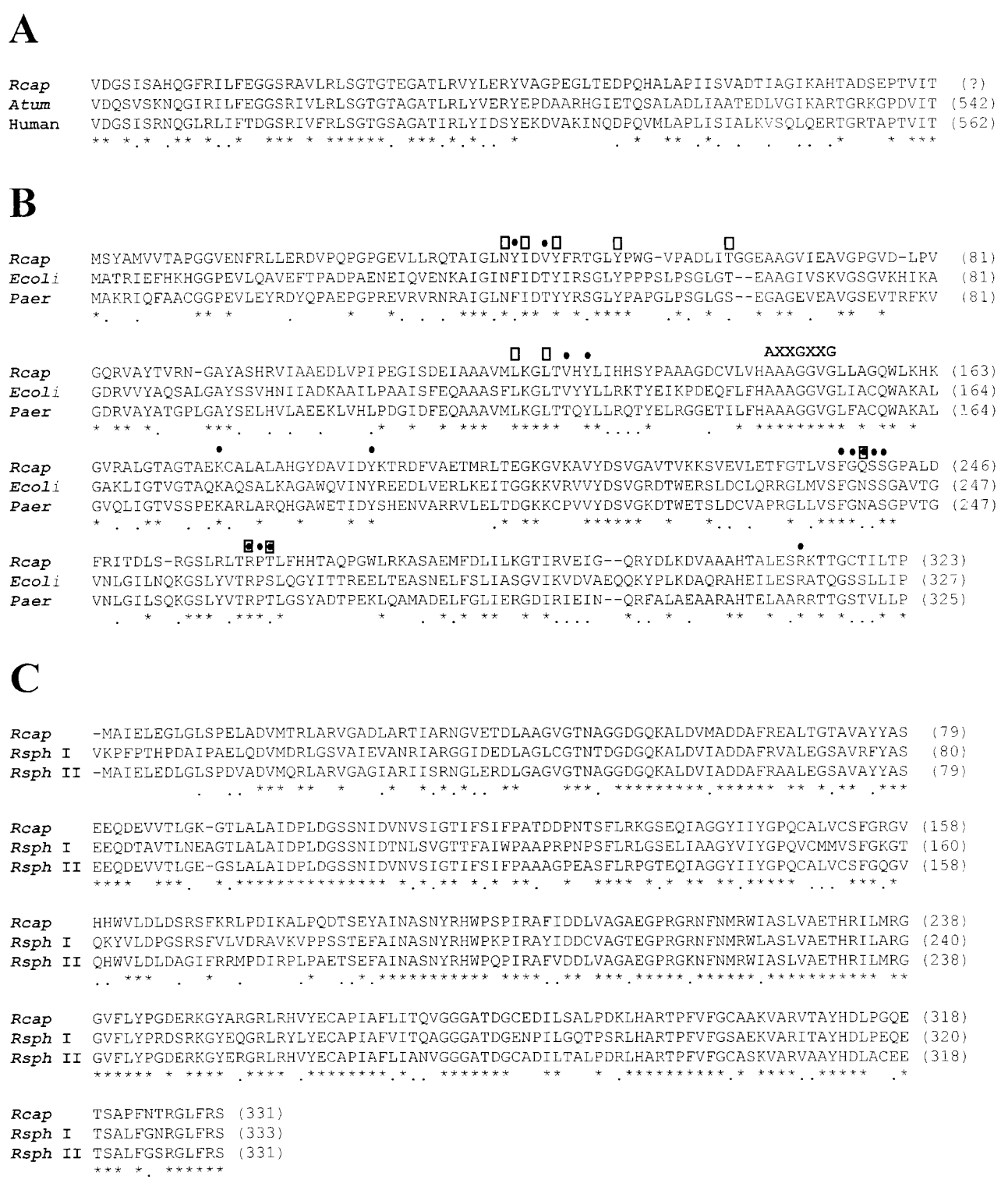

FIG. 2. Comparison and alignment of deduced amino acid sequences to sequences of known proteins. Invariant amino acids are indicated by asterisks and conservative changes are indicated by dots below the amino acids. (A) Alignment of the deduced amino acid sequence of the *R. capsulatus* (*Rcap*) partial ORF with that of *A. tumefaciens* (Atum) (51) and human phosphoglucomutase (58) amino acid sequences. In each case, the threonine residue is the C-terminal residue. (B) Amino acid sequence alignment of *R. capsulatus* QOR with QOR from *E. coli* (29) and *P. aeruginosa* (*Paer*) (GenBank accession no. X85015). AXXGXXG is an unusual nucleotide binding motif found in this protein (49). Additional residues in contact with the bound NADPH (●) and those that are within the catalytic site (□) are indicated. (C) FBPase amino acid alignment. The *R. capsulatus* deduced amino acid sequence is aligned with the amino acid sequences of *R. sphaeroides* FBPase I (14) and FBPase II (13) (*Rsph* I and *Rsph* II). (D) PRK amino acid sequence alignment. The *R. capsulatus* PRK amino acid sequence is aligned with the amino acid sequences of *R. sphaeroides* PRK I (14) and PRK II (13) (*Rsph* I and *Rsph* II). The putative ATP binding domain is indicated by the shaded box, and the pyridine nucleotide binding site is indicated by the bar. Residues implicated in the *R. sphaeroides* form I enzyme in sugar phosphate binding (#) and catalysis (∧) are noted. (E) Alignment of the *R. capsulatus* (Rc) *cbbT* partial deduced amino acid sequence with *R. capsulatus* TktA (4) and *R. sphaeroides* (Rs) CbbT (13) sequences.

D

```
                                                    ^   #   #
Rcap     MSKKYPIISVVGSSGAGTSTVKATFDQIFRREGVKAVSIEGDAFHRFNRADMKAELERRYAAGDATFSHFSYEANALEDL (80)
Rsph I   MSKKHPIISVTGSSGAGTSTVKHTFDQIFRREGVKAVSIEGDAFHRFNRADMKAELDRRYAAGDATFSHFSYEANELKEL (80)
Rsph II  MSKKYPIISVVGSSGAGTSTVKNFEEQIFRREGVKSVSIEGDAFHRFNRADMKAELERRYAAGDATFSHFSYEANELKEL (80)
         **** ***** **********   .*********.*******************.****************** * .*

Rcap     ERVFREYGETGKGRTRRYVHDANESAKYGVEPGHFTDWAPFEEDTDLLFYEGLHGCVTNDQVNIAAHADLKIGVVPVINL (160)
Rsph I   ERVFREYGETGQGRTRTYVHDDAEAARTGVAPGNFTDWRDFDSDSHLLFYEGLHGAVVNSEVNIAGLADLKIGVVPVINL (160)
Rsph II  ERVFREYGETGRGRTRTYVHDDAEAARTGVAPGNFTQWAPFEDNSDLLFYEGLHGCVVNDEVNLVRHADLKLGVAPVINL (160)
         **********.**** ****  *.*. ** **.** *  *.  . *********.* * .**.   ****.** *****
                   ^
Rcap     EWIQKIHRDRAQRGYTTEAVTDVILRRMHAYVHCIVPQFSQTDINFQRVPVVDTSNPFITRWIPTPDESLIVIRFRNPRG (240)
Rsph I   EWIQKIHRDRATRGYTTEAVTDVILRRMHAYVHCIVPQFSQTDINFQRVPVVDTSNPFIARWIPTADESVVVIRFRNPRG (240)
Rsph II  EWIQKIHRDRAQRGYTTEAVTDVILRRMYAYVGCIVPQFSETDINFQRVPVVDTSNPFIARWIPTPDESLIVIRFKNPRG (240)
         ********** ********************** *** *******.*****************.***** ***..****.****

Rcap     IDFPYLTSMIHGSWMSRANSIVIPGNKQDLAMQLILTPLIERLVREGRRARA (292)
Rsph I   IDFPYLTSMIHGSWMSRANSIVVPGNKLDLAMQLILTPLIDRVVRESKVA-- (290)
Rsph II  IDCPYLTSMIAGSWMSRANSIVVPGNKQDLAMQLILTPLIERMVREARRARA (292)
         ** ******* **********.**** ************.*.*** . *
```

E

```
Rc CbbT   (1) MKDLDM-----AQETRMANAIRALAMDAVEQAKSGHPGMPMGMADVATVLF (46)
Rs CbbT   (1) MKDIGA-----AQETRMANAIRALAMDAVEKAKSGHPGMPMGMADVATVLF (46)
Rc TktA   (1) M-DLAALRAKTPDHWKLATAIRVLAIDAVQAANSGHPGMPMGMADVATVLF (51)
              * *.          ..*.*** **.***. * ********************
```

FIG. 2—*Continued.*

Presumably, the latter deduced amino acid sequence is encoded by a heterotrophic transketolase.

An inverted repeat preceded by a sequence which matches a consensus RNase E cleavage site [(G/A)AUU(A/U)] (5) was found to be present within the 83-nucleotide *cbbP-cbbT* intergenic region. Since the combination of a hairpin preceded by an RNase cleavage site has recently been shown to be sufficient for cleavage of *puf* mRNA by an RNase E-like enzyme in *R. capsulatus* (11), this potential RNase E cleavage site could function in cbb_{II} mRNA processing.

Construction and phenotypes of *R. capsulatus cbb* mutant strains. Strains SBI$^-$ (*cbbL*), SBII$^-$ (*cbbM*), SBI-II (*cbbL cbbM*), SBP$^-$ (*cbbP*), SBRI$^-$ ($cbbR_I$), and SBRII$^-$ ($cbbR_{II}$) were constructed as described in Materials and Methods. The ability of the wild-type and mutant strains to grow under photoheterotrophic, photoautotrophic, and chemoautotrophic conditions was determined on solid media, and the results are presented in Table 1.

Characterization and complementation of RubisCO-minus strains. Analysis of *R. sphaeroides cbbL* and *cbbM* mutant strains revealed that disruption of the gene(s) encoding one RubisCO led to enhanced levels of RubisCO gene transcription, greater amounts of RubisCO protein, and enhanced enzyme activity of the remaining RubisCO. Indeed, the observed level of activity met or exceeded that present in the wild-type strain (14). To determine if a similar compensatory regulatory effect occurred in *R. capsulatus*, RubisCO activities and protein levels were assessed in *cbbL* and *cbbM* strains. The disruption of the *cbbL* and *cbbM* genes in *R. capsulatus* SBI$^-$ and SBII$^-$, respectively, was confirmed by hybridization analyses of Southern blots (data not shown), and Western immunoblotting confirmed the lack of RubisCO protein corresponding to each mutated gene (Fig. 3). Unlike the wild-type strain, in which form II RubisCO is present in both photoheterotrophically and photoautotrophically grown cells (Fig. 3B, lanes 2 and 5), form II RubisCO was not present in extracts of either photoheterotrophically or photoautotrophically grown SBII$^-$ (Fig. 3B, lanes 4 and 7). Since wild-type strain SB1003 did not synthesize detectable levels of form I RubisCO under photoheterotrophic conditions (Fig. 3A, lane 2), the lack of form I RubisCO in strain SBI$^-$ was confirmed by Western blot analysis of extracts from photoautotrophically grown cells (Fig. 3A, lane 6). Despite the fact that form I RubisCO is not detectable in photo-

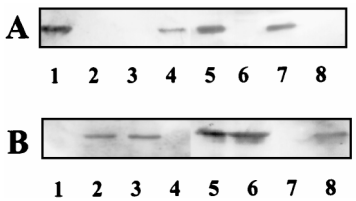

FIG. 3. Western immunoblot analysis of *R. capsulatus* wild-type and RubisCO-minus strains. Purified *Synechococcus* sp. strain PCC 6301 RubisCO and purified *R. sphaeroides* form II RubisCO were loaded into lanes 1 and 8, respectively. Crude extracts (approximately 10 μg of protein) were loaded as follows: lane 2, photoheterotrophically grown SB1003; lane 3, photoheterotrophically grown SBI$^-$; lane 4, photoheterotrophically grown SBII$^-$; lane 5, photoautotrophically grown SB1003; lane 6, photoautotrophically grown SBI$^-$; lane 7, photoautotrophically grown SBII$^-$. Blots were incubated with antibody raised against *Synechococcus* strain PCC 6301 RubisCO (A) and *R. sphaeroides* form II RubisCO (B). The figure was generated as follows: the region of interest of each blot was converted to TIFF files by using the software provide with the Molecular Dynamics Storm 840 imaging system (Molecular Dynamics), the TIFF files were imported into CorelDraw 7.0 (Corel Corporation, Ottawa, Ontario, Canada), where frames and numbers were added, and the images were printed on a Kodak ColorEase PS printer.

TABLE 2. Growth rates, RubisCO activities, and PRK activities of *R. capsulatus* wild-type and *cbb* mutant and complemented strains

Strain	Growth condition[a]	Doubling time[b] (h)	Activity (nmol min^{-1} mg^{-1})	
			RubisCO	PRK
SB1003 (wild type)	MAL	5.0	30.7 ± 16.5	112.9 ± 12.4
	PA	12.5	459.6 ± 51.0	451.1 ± 9.8
	MAL/DMSO	12.5	32.4 ± 8.4	95.3 ± 14.2
SBI$^-$ (*cbbL*)	MAL	6.5	51.3 ± 3.1	76.5 ± 15.7
	PA	15.5	362.8 ± 5.6	489.9 ± 36.2
SBII$^-$ (*cbbM*)	MAL	7.0	31.7 ± 1.3	193.0 ± 25.3
	PA	15.5	313.6 ± 18.4	506.3 ± 28.9
SBI-II (*cbbL*$^-$ *cbbM*)	MAL/DMSO	14.5	0.0	25.7 ± 5.8
SBI-II(pRPSFI-I)	MAL	9.5	34.5 ± 0.4	ND[c]
	PA	49.5	269.4 ± 13.9	ND
SBI-II(pRPSFII-I)	MAL	10.5	29.8 ± 4.9	ND
	PA	40.0	492.8 ± 39.2	ND
SBP$^-$ (*cbbP*)	MAL/DMSO	8.0	3.0 ± 1.1	0.0
SBP$^-$(pRPS::RsP_IA)	MAL	16.5	12.8 ± 1.8	922.8 ± 202.4
SBRI$^-$ (*cbbR*$_I$)	MAL	3.3	19.2 ± 0.6	ND
	PA	13.3	237.8 ± 33.7	ND
SBRI$^-$(pVK::CbbRI)	MAL	2.9	16.2 ± 0.7	ND
	PA	12.6	256.4 ± 21.5	ND
SBRII$^-$ (*cbbR*$_{II}$)	MAL	10.5	10.1 ± 1.9	11.3 ± 1.3
SBRII$^-$(pVK::CbbRII)	MAL	7.5	11.8 ± 0.1	17.8 ± 3.4
	PA	47.0	49.1 ± 3.5	64.5 ± 6.9

[a] MAL, photoheterotrophic growth on malate; PA, photoautotrophic growth on 1.5% CO_2–98.5% H_2; MAL/DMSO, photoheterotrophic growth on malate in the presence of 30 mM DMSO.

[b] Average of at least two independent determinations, with no more than a 15% discrepancy for any one growth rate.

[c] ND, not determined.

heterotrophically grown wild-type cells, either form I (strain SBII$^-$) or form II (SBI$^-$) RubisCO supported photoheterotrophic, photoautotrophic, and chemoautotrophic growth (Table 1); however, the doubling times for the mutant strains were slightly longer than for the wild-type under photoheterotrophic and photoautotrophic conditions (Table 2).

Strain SBII$^-$, which was unable to make form II RubisCO, was capable of photoheterotrophic growth. Apparently the lack of form II RubisCO synthesis resulted in the compensatory synthesis of form I RubisCO under photoheterotrophic conditions (Fig. 3A, lane 4). The level of RubisCO activity in photoheterotrophically grown strain SBII$^-$, which must be attributed to only form I RubisCO, was approximately the same as that observed for photoheterotrophically grown wild-type strain (Table 2). Likewise, the activity of form II RubisCO in photoheterotrophically grown SBI$^-$ was similar to but somewhat higher than that observed for the wild-type strain. Under photoautotrophic growth conditions, the levels of activity for the two RubisCO mutants approached that obtained in the wild-type strain (Table 2). This sort of compensation in RubisCO activity is analogous to that observed in *R. sphaeroides* form I or form II RubisCO-minus strains (14). The level of PRK activity in strains SBI$^-$ and SBII$^-$ did not vary significantly from that in the wild-type strain under either photoheterotrophic or photoautotrophic conditions (Table 2).

We constructed a strain lacking both forms of RubisCO (SBI-II) to determine if the CBB pathway was absolutely required for CO_2 fixation during photosynthetic and chemoautotrophic growth of *R. capsulatus* and whether this strain had the potential to serve as a host for recombinant RubisCO synthesis. *R. capsulatus cbbL cbbM* strain SBI-II was unable to grow autotrophically or photoheterotrophically in the absence of an alternate electron acceptor (Table 1) but could grow photoheterotrophically on malate with a doubling time of 14.5 h when DMSO was supplied as an alternate electron acceptor (Table 2). Despite the fact that DMSO did not have a significant effect on RubisCO or PRK activity in the wild-type strain (Table 2), strain SBI-II lacked detectable RubisCO activity when grown photoheterotrophically on malate with DMSO (Table 2), and neither form I nor form II RubisCO was detectable in extracts from these cultures (data not shown). Strain SBI-II exhibited PRK activity, but at a reduced level compared to strains SB1003, SBI$^-$, and SBII$^-$ (Table 2). *R. capsulatus* SBI-II could be complemented to photoheterotrophic and photoautotrophic growth with the *R. capsulatus cbbLS* or *cbbM* gene in plasmid pRPSFI-I or pRPSFII-I, respectively. Although RubisCO activity levels of the complemented strains were comparable to those in the wild-type strain, the complemented strains grew much more slowly than strain SB1003, particularly under photoautotrophic conditions (Table 2), similar to the situation with *R. sphaeroides* (7).

Characterization and complementation of the PRK-minus strain. Unlike *R. sphaeroides*, *R. capsulatus* appears to have only a single copy of *cbbP* (39). Further evidence that there is only one copy of *cbbP* in *R. capsulatus* was provided by low-stringency Southern blot analysis of *R. capsulatus* genomic DNA, using a probe derived from the *R. capsulatus cbbP* gene. In each case, the size of the hybridizing fragment corresponded to the size predicted for *cbbP*-containing fragment for the *cbb FPTGAM* region (data not shown). Hybridization and wash conditions were used such that a second copy of *cbbP* would be predicted to be less than 60% identical to the *cbbP* probe. PRK is the only enzyme, other than RubisCO, that is unique to the CBB pathway; therefore, disruption of the *R. capsulatus cbbP* gene should abolish the CBB pathway. In addition, if the *R. capsulatus cbbFPTGAM* genes form an operon, disruption of *cbbP* would be expected to have a polar effect on the expression of downstream genes, including *cbbM*. The *cbbP* deletion strain, SBP$^-$, was unable to grow photoautotrophically or chemoautotrophically and grew photoheterotrophically only when DMSO was supplied as an exogenous electron acceptor (Table 1). Strain SBP$^-$ lacked detectable PRK activity when grown photoheterotrophically with DMSO (Table 2) despite the fact that the presence of DMSO did not significantly reduce the level of PRK activity in the wild-type strain (Table 2). Additionally, Western immunoblot analysis showed low but detectable amounts of PRK in extracts from strain SB1003 grown photoheterotrophically in the presence of DMSO, while strain SBP$^-$ lacked detectable levels of PRK protein (Fig. 4C, lanes 1 and 2). A concomitant loss of detectable levels of form II RubisCO protein was also observed in SBP$^-$ (Fig. 4B, lanes 1 and 2). The level of RubisCO activity in strain SBP$^-$ grown photoheterotrophically in the presence of DMSO was much lower than that in wild-type strain SB1003 (Table 2), and unlike in strain SBII$^-$, the compensatory synthesis of form I RubisCO was not observed (Fig. 4A, lane 2). Complementation of *R. capsulatus* SBP$^-$ with *R. sphaeroides* $cbbP_I$ in expression vector pRPS-1 (pRPS::RsP_I) resulted in photoheterotrophic growth without a requirement for DMSO. Complementation was dependent on the proper orientation of the inserted DNA fragment. Despite very high PRK activity and PRK protein synthesis in the complemented strain (Table 2; Fig. 4C, lane 3), plasmid pRPS::RsP_I did not complement strain SBP$^-$ to photoautotrophic growth. A fourfold increase in RubisCO activity was also noted when strain SBP$^-$ was complemented with plasmid pRPS::RsP_I, and only form I RubisCO protein was detected (Table 2; Fig. 4A and B, lane 3). The loss of form II RubisCO protein in strain SBP$^-$ and the synthesis of only form I RubisCO in the complemented strain provide additional evidence that the cbb_{II} genes are cotranscribed.

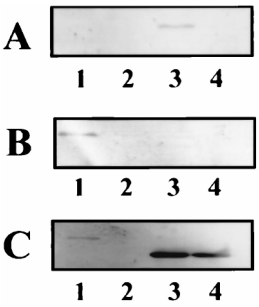

FIG. 4. Western blot analysis the *R. capsulatus* wild-type and PRK-minus strains. Crude extracts were prepared and loaded (approximately 10 μg of protein) as follow: lane 1, SB1003 grown photoheterotrophically with malate in the presence of DMSO; lane 2, SBP$^-$ grown photoheterotrophically with malate in the presence of DMSO; lane 3, strain SBP$^-$ with plasmid pRPS::RsP_I grown photoheterotrophically with malate; lane 4, purified *R. sphaeroides* PRK I. Blots were incubated with antibody raised against *Synechococcus* strain PCC 6301 RubisCO (A), *R. sphaeroides* form II RubisCO (B), and *R. sphaeroides* PRK I (C). The figure was generated as described in the legend to Fig. 3.

Characterization and complementation of CbbR I- and CbbR II-minus strains. *R. capsulatus* strains in which *cbbR*$_I$ and *cbbR*$_{II}$ were insertionally inactivated were constructed to establish a physiological role for the respective *cbbR* gene products. A strain in which the *cbbR*$_I$ gene was disrupted, strain SBRI$^-$, exhibited no phenotype (Table 1), and under photoheterotrophic conditions, RubisCO activity in this strain was not significantly lower than the level in the wild-type strain (Table 2). Interestingly, about one-half of the wild-type RubisCO activity was detected in strain SBRI$^-$ grown under photoautotrophic conditions (Table 2). Since form I RubisCO is not synthesized in photoheterotrophically grown SB1003, these results (wild-type RubisCO activity under photoheterotrophic conditions and reduced RubisCO activity under photoautotrophic conditions) would be consistent with the absence of form I RubisCO synthesis in strain SBRI$^-$. Western immunoblot analysis confirmed that RubisCO activity in strain SBRI$^-$ was due solely to form II RubisCO synthesis (Fig. 5). Form II RubisCO synthesis in strain SBRI$^-$ was qualitatively similar to that in the wild-type strain under both photoheterotrophic and photoautotrophic conditions (Fig. 5B, lanes 2 to 5). As in the wild-type strain, no form I RubisCO was present in extracts prepared from photoheterotrophically grown SBRI$^-$ (Fig. 5A, lanes 2 and 4), but unlike wild-type strain SB1003, strain SBRI$^-$ did not synthesize form I RubisCO even under photoautotrophic conditions (Fig. 5A, lanes 3 and 5). Although a slight reaction with the anti-form I RubisCO is visible in Fig. 5A, lane 5, this was not due to the presence form I RubisCO in extracts of photoautotrophically grown SBRI$^-$ because the cross-reacting protein is of higher apparent molecular weight than the form I RubisCO and it was not detected in subsequent Western immunoblots (data not shown). Introduction of the *R. capsulatus cbbR*$_I$ gene into strain SBRI$^-$ on plasmid pVK::CbbRI restored the ability to synthesize high levels of form I RubisCO under photoautotrophic conditions (Fig. 5A, lane 7) without an apparent effect on form I RubisCO synthesis under photoheterotrophic conditions (Fig. 5A, lane 6).

A strain in which *cbbR*$_{II}$ was insertionally inactivated, SBRII$^-$, was unable to grow photo- or chemoautotrophically (Table 1) but grew photoheterotrophically on malate at a reduced rate (Table 2). RubisCO and PRK activities in the *cbbR*$_{II}^-$ strain were reduced to 33 and 10%, respectively, of the activity observed in photoheterotrophically grown wild-type strain SB1003 (Table 2). Form II RubisCO protein was barely detectable in strain SBRII$^-$ compared to wild-type strain SB1003 (Fig. 5B, lanes 2 and 8). Unlike the response in strain SBII$^-$ (Fig. 3A), there was no apparent synthesis of form I RubisCO in response to the drastically reduced levels of form II RubisCO in strain SBRII$^-$ (Fig. 5A, lane 8). Strain SBRII$^-$ was complemented to photoautotrophic growth by the *cbbR*$_{II}$ gene on plasmid pVK::CbbRII. Despite the ability to complement strain SBRII$^-$ to autotrophic growth, the introduction of plasmid pVK::CbbRII did not restore the PRK or RubisCO activities to wild-type levels under either photoheterotrophic or photoautotrophic conditions (Table 2), and the photoautotrophic growth rate of the complemented strain was severely reduced relative to the wild-type rate (Table 2). Lack of complementation to wild-type enzyme activities might be due to the presence of the *cbb*$_{II}$ promoter, but not the *cbb*$_{II}$ genes, on complementing plasmid pVK::CbbRII. Binding of CbbRII to the *cbb*$_{II}$ promoter on the plasmid could titrate the activator away from the chromosomal *cbb*$_{II}$ promoter without leading to productive transcription. The complementation of strain SBRII$^-$ by plasmid pVK::CbbRII restored form II RubisCO synthesis under photoheterotrophic conditions (Fig. 5B, lane 9), and both form I and form II RubisCO were synthesized in photoautotrophically grown strain SBRII$^-$(pVK::CbbRII) (Fig. 5A and B, lanes 10).

Analysis of *R. capsulatus cbb* promoter fusion constructs. Promoter fusions were constructed to further examine the regulation of the *cbb* operons under photoheterotrophic and photoautotrophic conditions. β-Galactosidase activity was measured in extracts from SB1003 containing plasmid-borne fusions of *lacZ* to *cbb*$_{Ip}$ and *cbb*$_{IIp}$ (Table 1; Fig. 6). Under photoheterotrophic conditions, β-galactosidase activity was nearly undetectable in strain SB1003 containing the *cbb*$_{Ip}$-*lacZ* fusion pXLB (Fig. 6), consistent with the finding that form I RubisCO was not detected in *R. capsulatus* grown photoheterotrophically on malate (Table 2; Fig. 3). In agreement with previous studies (39, 46) and data presented here (Table 2; Fig. 3), which show that form II RubisCO is synthesized under photoheterotrophic conditions, β-galactosidase activities in photoheterotrophically grown SB1003 containing a *cbb*$_{IIp}$-*lacZ* fusion (pXFB) indicated that transcription occurred from *cbb*$_{IIp}$ under these conditions (Fig. 6). Increased β-galactosidase activity was observed in photoautotrophically grown SB1003 harboring either pXLB or pXFB, suggesting that transcription from *cbb*$_{Ip}$ and *cbb*$_{IIp}$ is induced under photoautotrophic conditions.

The role of CbbR II as a transcriptional activator of *cbb*$_{II}$

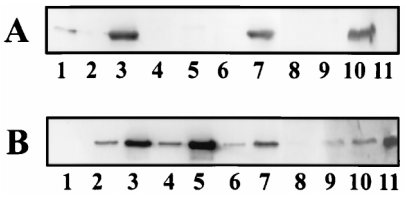

FIG. 5. Western immunoblot analysis of *R. capsulatus* wild-type and CbbR-minus strains. Purified *Synechococcus* sp. strain PCC 6301 RubisCO and purified *R. sphaeroides* form II RubisCO were loaded into lanes 1 and 11, respectively. Crude extracts were loaded (approximately 10 μg of protein) as follows: lane 2, photoheterotrophically grown SB1003; lane 3, photoautotrophically grown SB1003; lane 4, photoheterotrophically grown SBRI$^-$; lane 5, photoautotrophically grown SBRI$^-$; lane 6, photoheterotrophically grown SBRI$^-$ with pVK::CbbRI; lane 7, photoautotrophically grown SBRI$^-$ with pVK::CbbRI; lane 8, photoheterotrophically grown SBRII$^-$; lane 9, photoheterotrophically grown SBRII$^-$ with plasmid pVK::CbbRII; lane 10, photoautotrophically grown SBRII$^-$ with plasmid pVK::CbbRII. Blots were incubated with antibody raised against *Synechococcus* strain PCC 6301 RubisCO (A) and *R. sphaeroides* form II RubisCO (B). The figure was generated as described in the legend to Fig. 3.

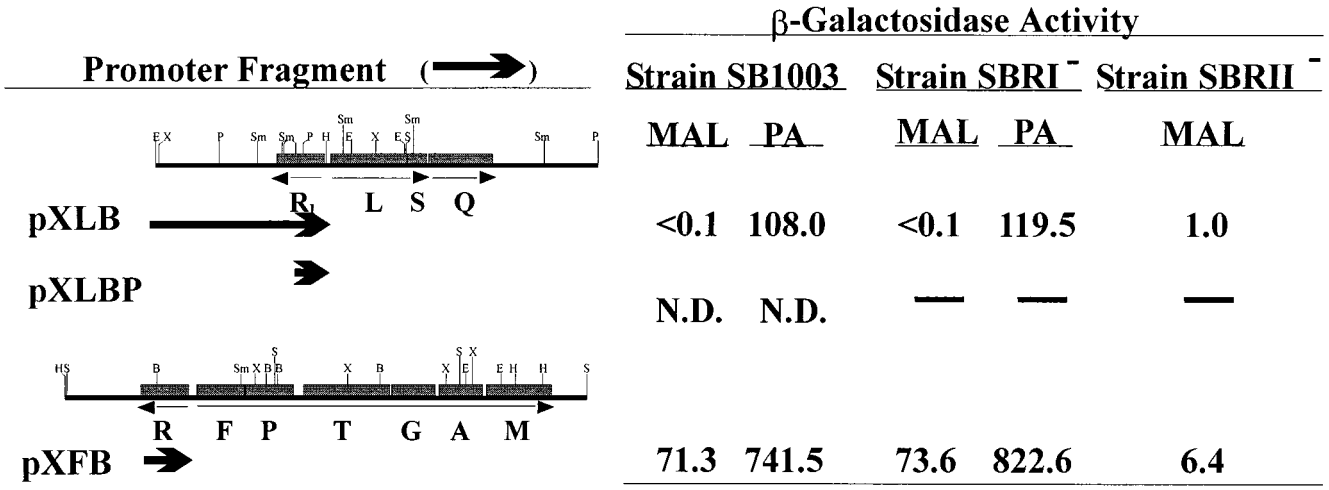

FIG. 6. β-Galactosidase activity from *R. capsulatus* cbb_P-*lacZ* fusions. The *cbb* promoter fragments that were fused to the *lacZ* gene in vector pXBA601 are represented by arrows. In plasmids pXLB and pXLBP, cbb_{IP} was fused to *lacZ* at the ATG start codon of *cbbL*. cbb_{IIP} was fused to the ATG start codon of *cbbF* in plasmid pXFB. β-Galactosidase activity is expressed in nanomoles/minute/milligram. The growth conditions were photoheterotrophically with malate as a carbon source (MAL) and photoautotrophically (PA). Strain SBRII$^-$ did not grow photoautotrophically, and so the β-galactosidase activity could not be determined. N.D., not detectable; —, not determined. The values are averages derived from multiple assays of two independent cultures for each strain.

was further established by measuring β-galactosidase activities in photoheterotrophically grown strain SBRII$^-$(pXFB). The level of β-galactosidase activity expressed from the cbb_{IIP} fusion construct in the $cbbR_{II}$ mutant strain was about 9% of that observed in the wild-type strain (Fig. 6). Any role for CbbR II in transcriptional activation at cbb_{IP} could not be addressed directly because the cbb_{IP}-*lacZ* fusion did not result in significant β-galactosidase activity in either strain SB1003 or strain SBRII$^-$, and the latter strain did not grow under photoautotrophic conditions. In addition, although a difference in β-galactosidase activity was observed in strains SB1003 and SBRII$^-$ containing pXLB, the activities were too low to determine if the differences were significant.

Direct evidence for transcriptional activation at cbb_{IP} by CbbR I could not be obtained by introducing the cbb_{IP}-*lacZ* fusions into strain SBRI$^-$. A cbb_{IP}-*lacZ* fusion containing a truncated $cbbR_I$ (pXLBP) was constructed (Table 1; Fig. 6) but did not yield detectable β-galactosidase in the wild-type strain even under photoautotrophic conditions (Fig. 6). β-Galactosidase activity in SBRI$^-$(pXLB) was similar to that measured in SB1003 containing plasmid pXLB (Fig. 6), but this was probably due to the complementation of strain SBRI$^-$ by the copy of the $cbbR_I$ gene on the promoter fragment in this construct. The levels of β-galactosidase activity in SBRI$^-$(pXFB) under photoheterotrophic and photoautotrophic growth conditions were very similar to or slightly higher than those measured in the wild-type strain containing pXFB (Fig. 6), suggesting that CbbR I does not act as a positive regulator at cbb_{IIP}.

DISCUSSION

Previous studies established that *cbb* gene organization in *R. capsulatus* is different from the situation for the *cbb* regulon of the closely related organism *R. sphaeroides* (38, 39). The present study elaborated additional features of *cbb* gene organization and control in *R. capsulatus* as a prelude to further detailed investigations of *cbb* regulation in this organism. The finding that the *cbbP* ribosomal binding site was within the *cbbF* coding region and the polar effect of the *cbbP* disruption on form II RubisCO synthesis provided strong evidence that the *R. capsulatus cbbFPTGAM* genes make up an operon (cbb_{II} operon). Moreover, the presence of a potential RNase E cleavage site within the *R. capsulatus cbbP-cbbT* intergenic region hints that posttranscriptional processing of the *R. capsulatus* cbb_{II} message may occur, reminiscent of the suggested posttranscriptional processing of *cbb* operon transcripts of *R. sphaeroides* (14). Despite these similarities, a very significant difference between the *R. capsulatus* and *R. sphaeroides* cbb_{II} operons is the presence of a *cbbR* gene, $cbbR_{II}$, divergently transcribed from the *R. capsulatus* cbb_{II} operon. In addition, a second *cbbR* gene, $cbbR_I$, is upstream and divergently transcribed from the *cbbLS* (cbb_I) operon. It has become well established that CbbR is involved in the regulation of *cbb* gene expression in a number of autotrophic bacteria, including *C. vinosum* (54), *Ralstonia eutropha* (formerly *Alcaligenes eutrophus*) (59), *Xanthobacter flavus* (34), *R. sphaeroides* (16), *Rhodospirillum rubrum* (8), and *Thiobacillus ferrooxidans* (26). These studies are buttressed by the finding that CbbR binds to the promoter region of the *cbb* operon (26, 27, 52, 53), with a physiological role for CbbR now well established (16, 52, 59). In *R. eutropha* (59), *R. sphaeroides* (16), and *X. flavus* (52), the product of a single *cbbR* gene regulates transcription from at least two different promoters. Consequently, transcription from these operons is coordinately activated within a single CbbR regulon. Only *Thiobacillus denitrificans* (30) and *R. capsulatus* have two potentially functional *cbbR* genes. The presence of two CbbR proteins in *R. capsulatus* raises questions concerning the involvement of each form of CbbR in the expression of the two or more *cbb* promoters found in this organism. The likelihood that CbbR I controls only the cbb_I operon was previously suggested since the $cbbR_I$, *cbbLS*, and *cbbQ* genes were all apparently acquired by horizontal gene transfer (38). Thus, to probe the role of the two CbbRs in *R. capsulatus cbb* gene regulation, strains with disruptions in $cbbR_I$ and $cbbR_{II}$ were constructed and characterized. A strain (SBRII$^-$) in which the $cbbR_{II}$ gene was disrupted was unable to grow autotrophically and grew at a reduced rate photoheterotrophically, showing reduced levels of both PRK and RubisCO activity and form II RubisCO protein. In addition, β-galactosidase activity derived from cbb_{IIP}-*lacZ* fusion pXFB in strain SBRII$^-$ was only about 9% of the activity of the

wild-type strain under photoheterotrophic conditions. These results clearly implicate CbbR II in activation of transcription at cbb_{IIp}. The presence of PRK activity in strain SBRII$^-$ indicates that some transcription from cbb_{IIp} occurred in the absence of CbbR II, albeit at an apparently reduced rate. Whether this was due to cross-talk activation by CbbR I remains to be established; however, it should be noted that transcription from cbb_{IIp} is not entirely dependent on CbbR in *R. sphaeroides* (16). The lack of form I RubisCO in photoautotrophically grown strain SBRI$^-$ provides evidence that CbbR I is involved in the regulation of form I RubisCO synthesis, probably by activating transcription at cbb_{Ip}. Furthermore, the absence of form I RubisCO in photoautotrophically grown strain SBRI$^-$ indicates that CbbR II is unable to activate transcription from cbb_{Ip}. In addition, the ability of strain SBRI$^-$ to grow under photoheterotrophic and autotrophic conditions, and the apparent normal level of form II RubisCO synthesis in this strain, demonstrate that CbbR I is not required for expression of the cbb_{II} operon. The data strongly indicate that the CbbR I and CbbR II proteins are necessary for normal regulation of the cbb_I and cbb_{II} operons, respectively, and that cross-talk activation of the *cbb* operons by the opposite CbbR protein does not occur. These studies thus provide the first indication that the *cbb* operons may belong to independent CbbR regulons.

LysR-type transcriptional activators generally bind to the promoter they activate, even under noninducing conditions, and the binding of a low-molecular-weight coinducer molecule to the LysR-type protein is required, in most cases, to activate transcription (45). It will be interesting to determine if independent regulation of the *R. capsulatus cbb* operons by the cognate CbbR proteins correlates with activation by unique coinducer molecules. Activation of transcription at cbb_{IIp} by CbbR II under photoheterotrophic conditions, and lack of transcriptional activation at cbb_{Ip} by CbbR I under the same conditions, indicate that either a repressor binds to cbb_{Ip} under photoheterotrophic conditions, different inducer molecules bind to the different CbbR proteins, or the CbbR proteins bind the same inducer with different affinities. In the latter case, it is possible that the intracellular concentration of the inducing metabolite increases under photoautotrophic conditions, resulting in activation of transcription at cbb_{Ip} by CbbR I. Certainly, the presence of two different CbbR proteins raises additional questions about DNA binding specificity. Since CbbR probably binds to the *cbb* promoter region in the absence of an inducer molecule, binding must be specific to prevent repressive effects on the opposite promoter (i.e., binding of CbbR II to the cbb_I promoter may not activate transcription but could prevent the binding of CbbR I). Current studies are directed at examining the specificity of CbbR I and CbbR II in vitro.

The product of the *qor* gene discovered downstream of $cbbR_{II}$ may also serve to regulate *cbb* gene expression. This gene encodes a soluble NAD(P)H QOR that catalyzes the reversible transfer of electrons from reduced pyridine nucleotides, with a preference for NADPH, to membrane-bound quinones. On the basis of the reaction catalyzed by this enzyme, QOR could function to sense or maintain the redox state of the membrane quinone pool. Interestingly, NADPH has been implicated as the coinducer of CbbR transcriptional activation in *X. flavus* (53). Thus, as a redox sensor, QOR could be involved in the regulation of *cbb* gene expression or perhaps in regulating the CBB pathway enzymes.

Although the evidence discussed above demonstrates that the cbb_I and cbb_{II} operons are differentially regulated by the two CbbR proteins, additional evidence suggests that regulation of these operons is also coordinated. When either *cbbM* or *cbbL* was disrupted, the absence of the missing RubisCO was compensated for, such that levels of RubisCO did not differ significantly from that in the wild-type strain. This compensation is analogous to what was observed in *R. sphaeroides* (14). However, the compensation effect was most dramatically demonstrated in *R. capsulatus* by the ability of strain SBII$^-$ to grow photoheterotrophically, concomitant with the synthesis of form I RubisCO. Since the wild-type strain did not synthesize detectable levels of form I RubisCO under photoheterotrophic conditions, the absence of form II RubisCO synthesis in strain SBII$^-$ somehow signaled the cell to compensate, by making form I RubisCO. However, compensation of form I RubisCO synthesis (Table 2) was not manifested by the *cbbP* mutant (strain SBP$^-$), in which form II RubisCO is not synthesized due to a polar effect of this mutation on *cbbM* (Fig. 4). These results thus suggest that the balance of various intermediates of the CBB pathway might regulate gene expression, which is an area that is currently being explored.

In summary, *R. capsulatus cbb* gene regulation is quite complex and differs markedly from that in *R. sphaeroides*. Two different CbbR transcriptional activators that allow autonomous regulation of the cbb_I and cbb_{II} operons, perhaps by binding different inducer molecules, are present in *R. capsulatus*. Obviously, to allow efficient regulation, the CbbR proteins must bind specifically to their respective *cbb* promoters. The presence of a potential RNase E recognition site within the cbb_{II} message suggests that it is posttranscriptionally processed. Further study of *R. capsulatus cbb* gene regulation will not only provide a better understanding of the control of CO_2 fixation but also address more general questions of gene regulation, such as the specificity of DNA-protein interactions and the significance of mRNA processing in prokaryotes.

ACKNOWLEDGMENTS

We thank J. T. Beatty for providing plasmid pXBA601 and Wenona Stankiewicz for technical assistance.

P.V. acknowledges the support provided by a Royal Thai graduate student scholarship. This work was supported by Public Health Service grant GM45404 from the National Institutes of Health.

REFERENCES

1. **Adams, C. W., M. E. Forrest, S. N. Cohen, and J. T. Beatty.** 1989. Structural and functional analysis of transcriptional control of the *Rhodobacter capsulatus puf* operon. J. Bacteriol. **171:**473–482.
2. **Ausubel, F. M., R. Brent, R. E. Kingston, D. D. Moore, J. G. Seidman, J. A. Smith, and K. Struhl (ed.).** 1987. Current protocols in molecular biology. Greene Publishing Associates and Wiley Interscience, New York, N.Y.
3. **Charlier, H. A., Jr., J. A. Runquist, and H. M. Miziorko.** 1994. Evidence supporting catalytic roles for aspartate residues in phosphoribulokinase. Biochemistry **33:**9343–9350.
4. **de Sury d'Aspremont, R., B. Toussaint, and P. M. Vignais.** 1996. Isolation of *Rhodobacter capsulatus* transketolase: cloning and sequencing of its structural *tklA* gene. Gene **169:**81–84.
5. **Ehretsmann, C. P., A. J. Carpousis, and H. M. Krisch.** 1992. Specificity of *Escherichia coli* endoribonuclease RNase E: *in vivo* and *in vitro* analysis of mutants in a bacteriophage T4 mRNA processing site. Genes Dev. **6:**149–159.
6. **Elhai, J., and C. P. Wolk.** 1988. A versatile class of positive-selection vectors based on the nonviability of palindrome-containing plasmids that allows cloning into long polylinkers. Gene **68:**119–138.
7. **Falcone, D. L., and F. R. Tabita.** 1991. Expression of endogenous and foreign ribulose 1,5-bisphosphate carboxylase-oxygenase (RubisCO) genes in a RubisCO deletion mutant of *Rhodobacter sphaeroides*. J. Bacteriol. **173:**2099–2108.
8. **Falcone, D. L., and F. R. Tabita.** 1993. Complementation analysis and regulation of CO_2 fixation gene expression in a ribulose 1,5-bisphosphate carboxylase/oxygenase deletion strain of *Rhodospirillum rubrum*. J. Bacteriol. **175:**5066–5077.

8a. **Falcone, D. L., and F. R. Tabita.** Unpublished data.

9. **Feinberg, A. P., and B. Vogelstein.** 1983. A technique for radiolabeling DNA restriction endonuclease fragments to high specific activity. Anal. Biochem. **132:**6–13.

10. **Figurski, D. H., and D. R. Helinski.** 1979. Replication of an origin-containing derivative of plasmid RK2 dependent on a plasmid function provided in trans. Proc. Natl. Acad. Sci. USA **76:**1648–1652.
11. **Fritsch, J. R., Rothfuchs, R. Rauhut, and G. Klug.** 1995. Identification of an mRNA element promoting rate-limiting cleavage of the polycistronic puf mRNA in *Rhodobacter capsulatus* by an enzyme similar to RNase E. Mol. Microbiol. **15:**1017–1029.
12. **Gibson, J. L.** 1995. Genetic analysis of CO_2 fixation genes, p. 1107–1124. *In* R. E. Blankenship, M. T. Madigan, and C. E. Bauer (ed.), Anoxygenic photosynthetic bacteria. Kluwer Academic Publisher, Dordrecht, The Netherlands.
13. **Gibson, J. L., J.-H. Chen, P. A. Tower, and F. R. Tabita.** 1990. The form II fructose 1,6-bisphosphatase and phosphoribulokinase genes form part of a large operon in *Rhodobacter sphaeroides*: primary structure and insertional mutagenesis analysis. Biochemistry **29:**8085–8093.
14. **Gibson, J. L., D. L. Falcone, and F. R. Tabita.** 1991. Nucleotide sequence, transcriptional analysis and expression of genes encoded within the form I CO_2 fixation operon of *Rhodobacter sphaeroides*. J. Biol. Chem. **266:**14646–14653.
15. **Gibson, J. L., and F. R. Tabita.** 1977. Isolation and preliminary characterization of two forms of ribulose 1,5-bisphosphate carboxylase from *Rhodopseudomonas capsulata*. J. Bacteriol. **132:**818–823.
16. **Gibson, J. L., and F. R. Tabita.** 1993. Nucleotide sequence and functional analysis of CbbR, a positive regulator of the Calvin cycle operons of *Rhodobacter sphaeroides*. J. Bacteriol. **175:**5778–5784.
17. **Gibson, J. L., and F. R. Tabita.** 1996. The molecular regulation of the reductive pentose phosphate pathway in proteobacteria and cyanobacteria. Arch. Microbiol. **166:**141–150.
18. **Gibson, J. L., and F. R. Tabita.** 1997. Analysis of the *cbbXYZ* operon of *Rhodobacter sphaeroides*. J. Bacteriol. **179:**663–669.
19. **Grimberg, J., S. Maguire, and L. Belluscio.** 1989. A simple method for the preparation of plasmid and chromosomal *E. coli* DNA. Nucleic Acids Res. **17:**8893.
20. **Hansen, T. A., and H. van Gemerden.** 1972. Sulfide utilization by purple nonsulfur bacteria. Arch. Microbiol. **86:**49–56.
20a. **Horken, K. M., and F. R. Tabita.** Unpublished data.
21. **Kay, R., and J. McPherson.** 1987. Hybrid pUC vectors for addition of new restriction enzyme sites to the ends of DNA fragments. Nucleic Acids Res. **15:**2778.
22. **Keen, N. T., S. Tamaki, D. Kobayashi, and D. Trollinger.** 1988. Improved broad-host-range plasmids for DNA cloning in Gram-negative bacteria. Gene **70:**191–197.
23. **Knauf, V. C., and E. Nester.** 1982. Wide host range cloning vectors: a cosmid bank of an *Agrobacterium* Ti plasmid. Plasmid **8:**45–54.
24. **Kreiger, T. J., L. Mende-Mueller, and H. M. Miziorko.** 1987. Phosphoribulokinase: isolation and sequence determination of the cysteine-containing active-site peptide modified by 5′-*p*-fluorosulfonylbenzoyladenosine. Biochim. Biophys. Acta **915:**112–119.
25. **Kreiger, T. J., and H. M. Miziorko.** 1986. Affinity labeling and purification of spinach leaf ribulose-5-phosphate kinase. Biochemistry **25:**247–252.
26. **Kusano, T., and K. Sugawara.** 1993. Specific binding of *Thiobacillus ferrooxidans* RbcR to the intergenic sequence between the *rbc* operon and the *rbcR* gene. J. Bacteriol. **175:**1019–1025.
27. **Kusian, B., and B. Bowien.** 1995. Operator binding of the CbbR protein, which activates the duplicate *cbb* CO_2 assimilation operons of *Alcaligenes eutrophus*. J. Bacteriol. **177:**6568–6574.
28. **Laemmli, U. K.** 1970. Cleavage of structural proteins during the assembly of the head of bacteriophage T4. Nature (London) **227:**680–685.
29. **Lilley, P. E., N. P. J. Stamford, S. G. Vasudevan, and N. E. Dixon.** 1993. The 92-min region of the *Escherichia coli* chromosome: location and cloning of the *ubiA* and *alr* genes. Gene **129:**9–16.
30. **Lorbach, S. C., and J. M. Shively.** 1995. Identification, isolation, and sequencing of the ribulose bisphosphate carboxylase/oxygenase regulatory genes (*cbbRI* and *cbbRII*) in *Thiobacillus denitrificans*, abstr. H207, p. 528. *In* Abstracts of the 95th General Meeting of the American Society for Microbiology 1995. American Society for Microbiology, Washington, D.C.
31. **Madigan, M. T., and H. Gest.** 1979. Growth of the photosynthetic bacterium *Rhodopseudomonas capsulata* chemoautotrophically in darkness with H_2 as the energy source. J. Bacteriol. **137:**524–530.
32. **Markwell, M. A. K., S. M. Haas, L. L. Bieber, and N. E. Tolbert.** 1978. A modification of the Lowry procedure to simplify protein determination in membrane and lipoprotein samples. Anal. Biochem. **87:**206–210.
33. **Mead, D. A., E. Szczesna-Skorupa, and B. Kemper.** 1986. Single-stranded DNA 'blue' T7 promoter plasmids: a versatile tandem promoter system for cloning and protein engineering. Protein Eng. **1:**67–74.
34. **Meijer, W. G., A. C. Arnberg, H. G. Enequist, P. Terpstra, M. E. Lidstrom, and L. Dijkhuizen.** 1991. Identification and organization of the carbon dioxide fixation genes in *Xanthobacter flavus* H4-14. Mol. Gen. Genet. **225:**320–330.
35. **Meijer, W. G., and F. R. Tabita.** 1992. Isolation and characterization of the *nifUSVW-rpoN* gene cluster from *Rhodobacter sphaeroides*. J. Bacteriol. **174:**3855–3866.
36. **Miller, J. H.** 1972. Experiments in molecular genetics, p. 352–355. Cold Spring Harbor Laboratory, Cold Spring Harbor, N.Y.
36a. **Novak, J. S., and F. R. Tabita.** Unpublished data.
37. **Ormerod, J. G., K. S. Ormerod, and H. Gest.** 1961. Light-dependent utilization of organic compounds and photoproduction of molecular hydrogen by the photosynthetic bacteria; relationships with nitrogen metabolism. Arch. Biochem. Biophys. **94:**449–463.
38. **Paoli, G. C., F. Soyer, J. M. Shively, and F. R. Tabita.** 1998. *Rhodobacter capsulatus* genes encoding form I ribulose-1,5-bisphosphate carboxylase/oxygenase (*cbbLS*) and neighbouring genes were acquired by a horizontal gene transfer. Microbiology **144:**219–227.
39. **Paoli, G. C., N. Strom-Morgan, J. M. Shively, and F. R. Tabita.** 1995. Expression of the *cbbLcbbS* and *cbbM* genes and distinct organization of the *cbb* Calvin cycle structural genes of *Rhodobacter capsulatus*. Arch. Microbiol. **164:**396–405.
40. **Penfold, R. J., and J. M. Pemberton.** 1992. An improved suicide vector for construction of chromosomal insertion mutations in bacteria. Gene **118:**145–146.
41. **Prentki, P., and H. M. Krisch.** 1984. In vitro insertional mutagenesis with a selectable DNA fragment. Gene **29:**303–313.
42. **Pridmore, R. D.** 1987. New and versatile cloning vectors with kanamycin-resistance marker. Gene **56:**309–312.
43. **Richardson, D. J., G. F. King, D. J. Kelly, A. G. McEwan, S. J. Ferguson, and J. B. Jackson.** 1988. The role of auxiliary oxidants in maintaining redox balance during growth of *Rhodobacter capsulatus* on propionate and butyrate. Arch. Microbiol. **150:**131–137.
44. **Sandbaken, M. G., J. A. Runquist, J. T. Barbieri, and H. M. Miziorko.** 1992. Identification of the phosphoribulokinase sugar phosphate binding domain. Biochemistry **31:**3715–3719.
45. **Schell, M. A.** 1993. Molecular biology of the LysR family of transcriptional regulators. Annu. Rev. Microbiol. **47:**597–626.
46. **Shively, J. M., E. Davidson, and B. L. Marrs.** 1984. Depression of the synthesis of the intermediate and large forms of ribulose-1,5-bisphosphate carboxylase/oxygenase in *Rhodopseudomonas capsulatus*. Arch. Microbiol. **138:**233–236.
47. **Tabita, F. R.** 1980. Pyridine nucleotide control and subunit structure of phosphoribulokinase from photosynthetic bacteria. J. Bacteriol. **143:**1275–1280.
48. **Tabita, F. R.** 1995. The biochemistry and molecular regulation of carbon metabolism and CO_2 fixation in purple bacteria, p. 885–914. *In* R. E. Blankenship, M. T. Madigan, and C. E. Bauer (ed.), Anoxygenic photosynthetic bacteria. Kluwer Academic Publishers, Dordrecht, The Netherlands.
49. **Thorn, J. M., J. D. Barton, N. E. Dixon, D. L. Ollis, and K. J. Edward.** 1995. Crystal structure of the *Escherichia coli* quinone oxidoreductase complexed with NADPH. J. Mol. Biol. **249:**785–799.
50. **Towbin, H., T. Staehelin, and J. Gordon.** 1979. Electrophoretic transfer of proteins from polyacrylamide gels to nitrocellulose sheets: procedure and some applications. Proc. Natl. Acad. Sci. USA **76:**4350–4354.
51. **Uttaro, A. D., and R. S. Ugalde.** 1994. A chromosomal cluster of genes encoding ADP-glucose synthetase, glycogen synthase, and phosphoglucomutase in *Agrobacterium tumefaciens*. Gene **150:**117–122.
52. **van den Bergh, E. R. E., L. Dijkhuizen, and W. G. Meijer.** 1993. CbbR, a LysR-type transcriptional activator, is required for expression of the autotrophic CO_2 fixation enzymes of *Xanthobacter flavus*. J. Bacteriol. **175:**6097–6104.
53. **van Keulen, G., L. Girbal, E. R. E. van den Bergh, L. Dijkhuizen, and W. G. Meijer.** 1998. The LysR-type transcriptional regulator CbbR controlling autotrophic CO_2 fixation by *Xanthobacter flavus* is an NADPH sensor. J. Bacteriol. **180:**1141–1147.
54. **Viale, A. M., H. Kobayashi, T. Akazawa, and S. Henikoff.** 1991. *rbcR*, a gene coding for a member of the LysR family of transcriptional regulators, is located upstream of the expressed set of ribulose 1,5-bisphosphate carboxylase/oxygenase genes in the photosynthetic bacterium *Chromatium vinosum*. J. Bacteriol. **173:**5224–5229.
55. **Wallenfels, K.** 1962. β-Galactosidase (crystalline). Methods Enzymol. **5:**212–219.
56. **Wang, X., D. L. Falcone, and F. R. Tabita.** 1993. Reductive pentose phosphate-independent CO_2 fixation in *Rhodobacter sphaeroides* and evidence that ribulose bisphosphate carboxylase/oxygenase activity serves to maintain redox balance of the cell. J. Bacteriol. **175:**3372–3379.
57. **Weaver, K. E., and F. R. Tabita.** 1983. Isolation and partial characterization of *Rhodopseudomonas sphaeroides* mutants defective in the regulation of ribulose bisphosphate carboxylase/oxygenase. J. Bacteriol. **156:**507–515.
58. **Whitehouse, D. B., W. Putt, J. U. Lovegrove, K. Morrison, M. Hollyoake, M. F. Fox, D. A. Hopkinson, and Y. H. Edwards.** 1992. Phosphoglucomutase 1: complete human and rabbit mRNA sequences and direct mapping of this highly polymorphic marker on human chromosome 1. Proc. Natl. Acad. Sci. USA **89:**411–415.
59. **Windhovel, U., and B. Bowien.** 1991. Identification of *cfxR*, an activator gene

of autotrophic CO_2 fixation in *Alcaligenes eutrophus*. Mol. Microbiol. **5:**2695–2705.

60. **Yanisch-Perron, C., J. Vieira, and J. Messing.** 1985. Improved M13 phage cloning vectors and host strains; nucleotide sequence of the M13mp18 and pUC19 vectors. Gene **33:**103–119.
61. **Yen, H. C., and B. Marrs.** 1976. Map of genes for carotenoid and bacteriochlorophyll biosynthesis in *Rhodopseudomonas capsulatus*. J. Bacteriol. **126:** 619–629.
62. **Yokoyama, K., N. R. Hayashi, S. Y. C. H. Arai, Y. Igarashi, and T. Kodama.** 1995. Genes encoding RubisCO in *Pseudomonas hydrogenothermophila* are followed by a novel *cbbQ* gene similar to *nirQ* of the denitrification gene cluster from *Pseudomonas* species. Gene **153:**75–79.